Physical Communication 75 (2026) 103063

Contents lists available at ScienceDirect

Physical Communication

journal homepage: www.elsevier.com/locate/phycom

Full length article

LSTM-based deep reinforcement learning for ISI mitigation in maritime LoRaWAN

Martine Lyimo *, Bonny Mgawe, Judith Leo, Mussa Dida, Kisangiri Michael

School of Computational and Communication Science and Engineering (CoCSE), The Nelson Mandela African Institution of Science and Technology (NM-AIST), Arusha 2331, Tanzania

ARTICLE INFO

Keywords:
LoRaWAN
inter-symbol interference (ISI)
maritime IoT
adaptive modulation and coding (AMC)
deep reinforcement learning (DRL)
long short-term memory (LSTM)
deep deterministic policy gradient (DDPG)
energy efficiency

ABSTRACT

For reliable, long-range, low-power Maritime Internet of Things (MIoT) communication (e.g., vessel tracking, ocean monitoring, and offshore automation), LoRaWAN offers attractive coverage and energy efficiency. However, sea-surface reflections, wave motion, and platform mobility create time-varying multipath with large delay spread, which induces inter-symbol interference (ISI) and degrades packet delivery ratio (PDR) and energy performance. This paper proposes a Long Short-Term Memory (LSTM)-assisted Deep Reinforcement Learning (DRL) framework LSTM–DDPG Adaptive Modulation and Coding (LD-AMC) that proactively mitigates ISI by predicting short-term channel evolution and adapting the LoRaWAN physical-layer parameters. An LSTM predictor learns temporal correlations in observed link metrics (RSSI, SNR, PER, and RMS delay spread) and provides one-step-ahead forecasts, which are appended to the agent state. A Deep Deterministic Policy Gradient (DDPG) controller then selects the spreading factor (SF), coding rate (CR), bandwidth (BW), and transmit power (P_t) within LoRaWAN constraints to maximize a reward that favors reliable delivery and throughput while penalizing energy cost and ISI severity. MATLAB/Simulink simulations under coastal and offshore two-ray maritime channels show that LD-AMC reduces ISI-induced symbol errors by up to 58%, improving PDR by up to 47% and reducing energy per delivered packet by up to 32% compared with standard and enhanced ADR baselines.

1. Introduction

Maritime Internet of Things (MIoT) applications such as vessel tracking, environmental monitoring, and offshore infrastructure surveillance are growing rapidly. These use cases demand wireless technologies that can offer reliable, long-range connectivity while maintaining low energy consumption, often under harsh and highly variable channel conditions at sea [1]. Low-Power Wide Area Networks (LPWANs) are well suited to this use case, offering low energy consumption and long-range coverage over unlicensed bands, using simple, asynchronous protocols [2].

Despite the advantages of LPWANs, the link between a Long-range Wide Area Network (LoRaWAN) node and the network server (Gateway) at sea remains problematic. The sea surface and the vessels are always moving, and this constant motion creates multiple reflected paths, time-varying delays, and Doppler shifts, all of which can distort the signal and reduce link reliability. These effects give rise to pronounced inter-symbol interference (ISI), which degrades the performance of spread spectrum links such as LoRa [3]. ISI significantly degrades communication performance because delayed echoes cause consecutive symbols to overlap, especially at low SFs where symbol durations are short [4].

Existing LoRaWAN mechanisms, such as Adaptive Data Rate (ADR), adjust the spreading factor (SF), bandwidth (BW), coding rate (CR), and transmit power (Pt) based on average link conditions. However, ADR is mostly reactive and does not anticipate how the maritime channel will change over time. This makes it less effective in highly dynamic scenarios, such as fast-moving vessels or rough sea states, where it struggles to prevent ISI and to maintain a consistent quality of service [5].

One way to close this gap is to use intelligent adaptation of modulation and coding, commonly referred to as Adaptive Modulation and Coding (AMC). In terrestrial wireless systems, including 4 G and 5 G, AMC dynamically selects modulation schemes and coding rates using instantaneous channel state information (CSI) [6]. More recently, similar ideas have been applied to LoRa-based links, where integrating AMC with machine learning–driven channel awareness has been shown

* Corresponding author.
E-mail address: martine.lyimo@nm-aist.ac.tz (M. Lyimo).

https://doi.org/10.1016/j.phycom.2026.103063
Received 11 February 2026; Accepted 27 February 2026
Available online 28 February 2026

to improve both throughput and reliability [7]. However, although channel awareness is inherently related to ISI, most existing AMC studies for LoRa/LoRaWAN do not explicitly model or optimize against ISI, and their reactive CSI assumptions remain inadequate for rapidly time-varying maritime channels.

Traditional LoRaWAN infrastructures usually use static or semi-adaptive settings, with an ADR algorithm that adapts the SF, BW, and CR parameters based on link quality indicators such as Received Signal Strength Indicator (RSSI) and Signal-to-Noise Ratio (SNR) [8]. This works well in terrestrial environments with stable channel conditions; however, it does not work well when channel conditions change rapidly, as in a maritime climate, where sea state, vessel motion, tides, and weather can rapidly alter the channel [9,10]. The reactive nature of the ADR, in conjunction with its relatively low uplink update rate, makes it poor in dealing with fast-fading multipath effects, in particular when the channel delay spread is on the order of, or larger than, the symbol duration, leading to substantial ISI. The performance of traditional ADR in retaining high PDR and energy efficiency is severely affected in such maritime scenarios, especially at low SFs [11].

In this paper, we propose an ISI-aware adaptive modulation and coding framework, termed LSTM–DDPG Adaptive Modulation and Coding (LD-AMC), for maritime LoRaWAN links. The primary objective is to proactively reduce ISI by anticipating short-term channel variation; throughput and energy are included in the objective because LoRaWAN is strongly energy-constrained and ISI-mitigation actions (e.g., higher SF or stronger coding) directly trade off with airtime and battery life. A two-ray-based maritime LoRaWAN channel and delay-spread model that captures the dominant direct and sea-surface reflected components and their time variation under wave motion and mobility, enabling ISI-oriented analysis.

DRL has been widely applied to optimize wireless transmission parameters and link adaptation policies [12]. However, many of these studies do not explicitly model maritime over-sea propagation, where strong sea-surface reflections produce a pronounced two-ray effect and rapidly varying channel behaviour [13]. In this work, we move beyond generic parameter tuning by combining LSTM-based short-term prediction of channel/ISI evolution with DDPG-based LD-AMC control to proactively select LoRaWAN PHY parameters under practical time-on-air and energy constraints. This prediction-assisted, ISI-aware design enables more stable and reliable adaptation in rapidly changing maritime conditions than purely reactive or SNR-threshold-based schemes.

The main contributions of this paper are;

- A two-ray-based maritime LoRaWAN channel and delay-spread model that captures the dominant direct and sea-surface reflected components and their time variation under wave motion and mobility, enabling ISI-oriented analysis.
- An LD-AMC control scheme that integrates LSTM-based prediction of short-term channel/ISI indicators with a Deep Deterministic Policy Gradient (DDPG) controller to adapt SF, CR, BW, and P_t in real time within LoRaWAN constraints.
- A simulation-based evaluation in coastal and offshore scenarios showing consistent gains over standard and enhanced ADR baselines in terms of ISI-induced symbol errors, PDR, and energy per delivered packet.

The rest of the paper is structured as follows. Section 2 reviews prior work on LoRaWAN in marine environments and on adaptive modulation and coding schemes for time-varying wireless channels. In Section 3, we describe our system model and problem statement, including a description of our maritime channel model and the effects of ISI. In Section 4, we describe our proposed LD-AMC scheme in detail and simulation setup in Section 5. The results from our simulations are provided in Section 6, followed by our conclusions and discussion of future work in Section 7.

2. Related works

2.1. LoRaWAN in maritime environments

Pensieri et al. [14] tested LoRaWAN aboard both commercial passenger and research vessels at sea, and in a variety of coastal and offshore water environments. Their experimental results demonstrate the impact of node movement and changing marine geometry on both signal stability and packet delivery. Nonetheless, they do not model delay spread or ISI directly; instead, they use packet loss, RSSI, and SNR to analyze their data. Therefore, these studies will not serve as a basis for developing advanced optimization and control strategies. In contrast to the limited body of work on ISI at the LoRa physical layer, a notable investigation is presented by Demeslay et al. [15]. However, that study does not address real-time strategies for ISI mitigation and is not combined with any adaptive modulation framework.

Parri et al. [16] evaluated LoRaWAN connectivity for offshore marine monitoring by deploying sensor nodes at sea and placing gateways along the coast. Their sea trials made it clear that both offshore distance and the way the nodes were arranged affected packet delivery, RSSI, and SNR, and they showed that LoRaWAN can, at least, support simple over-sea data collection. However, the study only reports high-level link metrics and does not look at delay spread or ISI in any detail. As a result, its findings are of limited use when trying to design more advanced, ISI-aware optimization and control schemes.

2.2. Limitations of traditional ADR algorithms

In LoRaWAN, ADR mainly tweaks the SF and transmit power based on the average SNR/RSSI measured at the network server. This is usually acceptable for mostly static end devices, but recent work has shown clear limits in more dynamic scenarios. Kufakunesu et al. report that standard ADR reacts slowly, assumes the channel is almost static, and can even reduce both PDR and energy efficiency when conditions change quickly [17]. Newer approaches, such as ND-ADR (which targets collision reduction in dense networks) and enhanced ADR schemes for mobile agricultural nodes, lead to the same overall conclusion: the original ADR mechanism needs substantial redesign to deal effectively with interference and mobility [18]. Although these approaches use coarse link-metric data (SNR, RSSI, PER), they do not explicitly address delay spread or ISI. Thus, they are not well-suited for the very severe multipath conditions typically experienced in maritime LoRaWAN links.

2.3. Emerging artificial intelligence (AI)-driven approaches

Carvalho et al. [19] deployed at the gateway, the agent uses SNR feedback from received packets to achieve the highest effective data delivery rate and the lowest energy consumption. The simulations in ns-3 showed that the proposed solution could outperform standard ADR, with time-on-air substantially lower and data efficiency higher. However, the proposed solution has been tested only in a static indoor environment. It does not account for delay spread, mobility, or ISI, which makes it irrelevant for maritime LoRaWAN deployments.

Sabna Thenginthody Hassan et al. [20] introduced a DNN receiver for underwater acoustic Orthogonal Frequency Division Multiplexing (OFDM) systems to address ISI in the context of complex multipath propagation. The authors have demonstrated an improvement in demodulation performance using their developed model, which learns nonlinear channel distortions, based on real river-trial measurements. In contrast to traditional linear equalizers, the authors' model was shown to be resilient to channel distortions; however, although the authors' model has been very successful in the context of underwater acoustic channels the same cannot be said for the LoRaWAN environment as their model is based on the OFDM waveform and the baseband acoustic signaling method, while LoRaWAN uses CSS signals.

Bagherian et al. [21] proposed an algorithm using machine learning to optimize LoRaWAN localization based on adjusting the BW, SF, and CR. and coding rate at the physical layer. Using regression models, they reported gains of up to about 60 % in positioning accuracy, showing that data-driven tuning of these parameters can make a clear difference in LPWAN systems. However, their work does not account for ISI or time-varying channel conditions; therefore, it has limited applicability to harsh or highly dynamic environments.

In Huang et al.'s research [22] the authors investigated whether machine learning can be used for AMC within underwater acoustic communication systems. In this research, the authors propose an AMC system based on a weighted k-nearest neighbors (w-kNN) classifier trained on real field-trial measurements of delay spread, SNR, and multipath characteristics. The results show the use of machine learning to improve BER stability and overall network throughput in highly variable, dynamically changing underwater channels affected by ISI. However, the authors' focus is on underwater acoustic communication systems; therefore, it is unclear how easily their solution could be adapted to RF-based maritime LoRaWAN networks.

Acosta-García et al. [23] applied the Q-learning strategy to create a dynamic transmission policy that adjusts the SF and P_t in real time based on changes in the network environment, thereby reducing the number of packet collisions and energy consumption. The proposed methodology is very efficient in dynamically controlling SF and P_t at the data-link layer; however, it does not provide a mechanism to predict or minimize ISI, which is a significant drawback given the large amount of multipath-induced delay spread and ISI found in most maritime environments.

Over recent years, several alternatives have emerged that use AI and RL to enhance LoRaWAN's adaptability. Although several of these approaches can enhance link optimization and resource allocation, most are not tailored to marine environments and do not explicitly account for ISI or the associated delay-spread characteristics.

RADR is an AI-based adaptive data rate scheme for LoRaWAN, proposed by Kim and Pyun, that uses a trained model to choose efficient data rates for mobile location-based services and significantly improves packet success rate compared with standard ADR [24]. However, RADR is designed for terrestrial mobile scenarios and does not consider key challenges of long over-sea links, such as strong multipath reflections and delay spread, so it is not directly suitable for maritime LoRaWAN.

Another recent variant is ND-ADR [18], which introduces a non-destructive scheduling strategy to reduce collisions and improve energy efficiency. However, it still lacks predictive channel modelling and does not perform adaptive modulation both important for coping with fast channel changes in maritime environments. In parallel, AI-ERA [25] uses deep neural networks (DNNs) to forecast short-term channel conditions and to select the SF for each transmission. This gives a smart, proactive way to adjust SF on a packet-by-packet basis. However, the method does not account for delay-spread effects, which are central to ISI and crucial for maintaining link reliability in more demanding environments.

Recent studies have shown that DRL can effectively optimize multiple parameters in complex wireless systems. For example, Wu et al. proposed a DRL-enabled optimization framework for RIS-assisted satellite–aerial–terrestrial integrated networks, highlighting trade-offs among spectral, secrecy and energy efficiency [26]. Similarly, federated-learning concepts have been used to enable distributed learning and multiple functionalities in satellite–terrestrial integrated networks while preserving privacy [27]. While these works demonstrate the strength of learning-based optimization, they address different network architectures and objectives; in contrast, our work targets maritime LoRaWAN, where time-varying excess delay and sea-surface reflections create ISI, and we therefore combine LSTM-based short-term prediction with DDPG-based LD-AMC control under LoRaWAN ToA and energy constraints.

2.4. Positioning with recent IoT, learning, and energy-efficiency research

Learning-enabled optimization is increasingly central to next-generation IoT connectivity, particularly in space–air–ground and other integrated networking paradigms where link conditions and service demands vary rapidly. For example, rate-splitting multiple access has been explored to enhance IoT support in satellite- and aerial-integrated networks [28], and AI-driven approaches have been emphasized as enablers of seamless, massive access in space–air–ground integrated networks [29]. In parallel, energy-aware and self-sustaining designs are increasingly important for constrained devices, including self-powered absorptive reconfigurable intelligent surfaces [30] and secrecy–energy efficient hybrid beamforming strategies in integrated satellite–terrestrial networks [31]. Motivated by these directions, this work targets energy-constrained maritime IoT and develops an LSTM-assisted DRL (LD-AMC) strategy that adapts LoRaWAN physical-layer parameters to mitigate ISI, while maintaining a practical balance between reliability, time-on-air, and power consumption.

2.5. Propagation models for marine ISI analysis

The ITU-R P.1411–10 recommendation [32] provides a two-ray ground-reflection model suited to short-range and over-water radio links. It captures the main features of delay spread in such environments. However, it is defined purely as a propagation model and is not linked to upper-layer adaptation or AI-based link control. As a result, it provides a useful basis for studying ISI in maritime channels, but on its own, it is insufficient for developing comprehensive ISI mitigation strategies. A summary of these contributions and remaining gaps is given in Table 1.

3. System model and problem formulation

3.1. Maritime channel model

Wireless maritime communication differs from terrestrial communication because a large fraction of the received energy comes from sea-surface reflections, propagation distances are often longer, and the geometry varies in time due to waves and vessel motion. These factors lead to strong multipath propagation, which in turn increases delay spread and gives rise to ISI in LoRaWAN links. To capture these effects, the wireless channel in this work is modelled using a two-ray maritime propagation model, in which the received signal is composed of a direct line-of-sight (LoS) component and a reflected component from the dynamically evolving sea surface.

For a transmission occurring at time t, the complex baseband channel response is expressed as

$$h(t) = \alpha_1\delta(t-\tau_1) + \alpha_2\delta(t-\tau_2)e^{i\phi} \tag{1}$$

where α_1 and α_2 denote the amplitudes of the direct and reflected paths, τ_1 and τ_2 are the respective propagation delays, and ϕ is the differential phase introduced by reflection. The reflection coefficient Γ is computed according to the sea-surface dielectric properties and grazing angle θ:

$$\Gamma(\theta) = \frac{\varepsilon_r \sin\theta - \sqrt{\varepsilon_r - cos^2\theta}}{\varepsilon_r \sin\theta + \sqrt{\varepsilon_r - cos^2\theta}} \tag{2}$$

With ε_r representing the complex permittivity of seawater. This time-varying channel response generates a power-delay profile (PDP) from which the Root Mean Square (RMS) delay spread is obtained and serves as the principal driver of ISI severity. This model reflects empirical findings from ITU-R P.1546 and COST-231-based maritime datasets [33], as well as recent literature on sea-surface channel modelling [34].

Wave-driven reflection variability and risk levels: In maritime links, wave motion and sea-surface roughness make the reflected component time-varying by altering the effective reflection magnitude and phase, as well as the excess path delay. We capture this using a time-

Table 1
Summary of related works in LoRaWAN research.

Reference	Research context	Methodology	Description	Research gap
[14]	Maritime LoRaWAN deployment	Field measurements & coverage analysis	Analyzes LoRaWAN signal coverage in marine conditions.	Lacks any adaptive or intelligent approach for ISI mitigation.
[15]	ISI modelling in the LoRa PHY layer	Semi-analytical error analysis combined with simulation	Evaluates symbol error rate (SER) under multipath conditions and quantifies ISI effects in LoRa receivers.	Does not provide real-time mitigation or link ISI modelling to any adaptive or intelligent control framework.
[19]	Static ADR optimization	Q-learning via ns-3 simulation	Optimized SF/TP to improve delivery and energy.	No ISI or maritime adaptation considered.
[20]	Underwater OFDM DNN receiver (river trial)	Deep neural network-based receiver	Validated a DNN-based OFDM receiver in river experiments, effectively mitigating severe multipath delay spread.	Tailored for underwater OFDM; not applicable to RF-based LoRaWAN ISI scenarios.
[21]	LoRaWAN localization	ML-based tuning of SF, BW, CR	Improves localization accuracy by using ML to adjust SF, BW, and CR, with gains of up to ∼60 %.	Not aimed at ISI or dynamic multipath; focuses only on positioning.
[22]	Underwater AMC with ML	ML-based AMC using w-kNN	Uses delay spread and multipath features to lower BER under ISI.	Designed for underwater acoustic channels, not for LoRaWAN RF links
[23]	LoRaWAN dynamic transmission policy	Q-learning for SF/TP adaptation	Adaptive SF/TP tuning to reduce energy and collisions.	No ISI or multipath modelling; not evaluated for maritime scenarios.
[24]	Reinforcement learning for ADR	Deep RL for ADR improvement	Applies reinforcement learning for adaptive rate control (RADR).	Not optimized for maritime delay spread and ISI.
[18]	Enhanced ADR using adaptive scheduling	Heuristic scheduling algorithm	ND-ADR dynamically tunes parameters while conserving node energy history.	Does not model channel variation or multipath-induced ISI.
[25]	AI-driven resource allocation in LoRaWAN	DNN prediction model for SF assignment	AI-ERA selects optimal SF using a DNN based on SNR and distance.	No integration of delay spread or ISI-aware learning mechanisms.
[32]	Delay spread modelling (marine)	Two-ray ground reflection model	Provides a two-ray reflection model for over-water signal paths.	Not integrated with adaptive link control.
[26]	RIS-assisted satellite–aerial–terrestrial integrated networks (SATIN)	DRL-based multi-parameter optimization (e.g., DDQN/DRL)	Optimizes multiple communication parameters to balance spectral, secrecy, and energy efficiency trade-offs in integrated networks	Not designed for maritime LoRaWAN; does not model sea-surface two-ray induced excess-delay variations and ISI, nor LoRaWAN ToA and power constraints
[27]	Satellite–terrestrial integrated networks	Federated learning–enabled framework	Uses federated learning concepts to enable distributed learning and multiple functionalities with privacy considerations	Focuses on federated multi-function frameworks rather than prediction-assisted PHY adaptation for ISI mitigation in maritime LoRaWAN; no explicit LSTM-assisted LD-AMC design under LoRaWAN constraints.
This Work (LD-AMC)	ISI-aware AMC for maritime LoRaWAN	LSTM-DDPG hybrid DRL framework	Proposes an intelligent LD-AMC model that dynamically adjusts LoRaWAN transmission parameters using DRL guided by LSTM-based channel prediction.	Bridges the gap by combining LSTM-based channel prediction with DDPG-driven AMC control, enabling real-time ISI mitigation in maritime multipath channels.

varying reflection coefficient

$$\Gamma(t) = \Gamma_0\,\eta(t)e^{j\phi(t)} \tag{3}$$

and a time-varying excess delay,

$$\Delta\tau(t) = \Delta d(t)/c \tag{4}$$

where $\eta(t)$ models coherence loss due to roughness and $\phi(t)$ models wave-induced phase fluctuations. Since ISI depends on the strength and delay of reflected components, variations in $\Gamma(t)$ and $\Delta\tau(t)$ directly translate into time-varying ISI severity. We therefore define three channel variability "risk levels": low (calm sea, small/slow variations), medium (moderate fluctuations), and high (rough sea, fast and large variations), which are used to generate and interpret different maritime conditions in the simulations.

Beyond two-ray, diffuse scattering and atmospheric attenuation: The two-ray model captures the dominant line-of-sight (LoS) and sea-surface reflection components that strongly influence excess delay and ISI in maritime links. However, real environments may also include additional weak multipath components caused by wave scattering, nearby vessels, and coastal structures. To reflect this, we represent the channel as the sum of a two-ray component and a diffuse multipath term,

$$\mathrm{h}(\mathrm{t},\tau) = \mathrm{h}_{2-\mathrm{ray}}(\mathrm{t},\tau) + \mathrm{h}_{\mathrm{diff}}(\mathrm{t},\tau) \tag{5}$$

where $h_{\mathrm{diff}}(t,\tau)$ models scattered paths with lower power and time-varying delays. In addition, maritime links may experience excess attenuation due to humidity, sea spray, and salt fog. This effect can be incorporated in the link budget as a time-varying excess-loss term $L_{\mathrm{fog}}(t)$, yielding

$$\mathrm{P_r}(\mathrm{t}) = \mathrm{P_t} + \mathrm{G_t} + \mathrm{G_r} - \left(\mathrm{L_{PL}}(\mathrm{t}) + \mathrm{L_{fog}}(\mathrm{t})\right) \tag{6}$$

where $L_{\mathrm{PL}}(t)$ denotes the propagation loss captured by the baseline model (including two-ray interference). In this work, the primary emphasis is on ISI behaviour driven by reflection-induced delay variations; therefore, $h_{\mathrm{diff}}(t,\tau)$ and $L_{\mathrm{fog}}(t)$ are treated as scenario-dependent variability terms and are highlighted as key extensions for measurement-based validation.

3.2. ISI analysis

ISI occurs when delayed signal echoes from different paths arrive so late that they overlap with the next symbol, causing detection errors. Over the sea, strong reflections from the water surface and moving platforms create time-varying multipath and non-negligible RMS delay spreads, as shown in recent over-the-sea channel studies and maritime measurements [13]. Suppose the delay spread becomes similar to or larger than the LoRa symbol duration. In that case, ISI becomes a dominant impairment, so controlling delay spread is a key requirement for a reliable maritime LoRaWAN link [35].

LoRa uses chirp spread-spectrum (CSS) modulation, where the SF determines the symbol duration. The symbol duration is

$$T_s = \frac{2^{SF}}{BW} \tag{7}$$

assuming a 125 kHz BW. Lower SFs generate short symbols and therefore provide higher spectral efficiency, but they are significantly more vulnerable to ISI in channels with large delay spread. Higher SFs produce longer symbols that better tolerate multipath distortion but incur greater latency and energy cost. This trade-off has been verified in LoRa PHY analyses under multipath conditions and in maritime field measurements [15].

Table 2 summarizes the symbol duration and corresponding ISI susceptibility for typical LoRaWAN settings. In this work, we approximate the ISI threshold as 1 % of the LoRa symbol duration T_s. This is a practical, heuristic choice: prior LoRa studies show that very small delays (a few percent of T_s barely affect BER, while larger fractions cause a sharp performance drop [36,37], and our simulations follow the same trend.

To quantify ISI severity, the RMS delay spread is used, and it is computed from the PDP.

$$\tau_{rms} = \sqrt{\frac{\sum_i P(\tau_i)(\tau_i - \tau_m)^2}{\sum_i P(\tau_i)}} \tag{8}$$

Where $P(\tau_i)$ is the PDP sample at delay τ_i, τ_{rms} is the RMS delay spread and τ_m is the mean delay:

$$\tau_m = \frac{\sum_i P(\tau_i)\tau_i}{\sum_i P\tau_i} \tag{9}$$

When τ_{rms} becomes a significant fraction of the symbol duration Ts. Symbol overlap occurs, and the channel enters an ISI-dominant regime. Such conditions are frequently observed in maritime channels where the two-ray component, influenced by sea-state variations and vessel motion, introduces delay spreads on the order of hundreds of microseconds [38].

These ISI characteristics highlight the need for intelligent, AMC schemes that can tune SF, CR, and BW as the delay spread changes. The ISI analysis above provides the analytical basis for the LD-AMC framework introduced later in this work, and it supports real-time, ISI-aware decisions using both measured and predicted channel statistics.

3.3. ADR and proposed LSTM-based ADR formulation

In conventional LoRaWAN ADR, the network uses recent uplink link-quality measurements to update the transmission settings. From the last L uplinks, it computes the average SNR and SNR margin Δ

$$\Delta = \overline{\mathrm{SNR}} - \mathrm{SNR}_{req}(\mathrm{SF}) - M \tag{10}$$

where $\mathrm{SNR}_{req}(\mathrm{SF})$ is the required SNR for the current spreading factor SF (from the receiver sensitivity/SNR threshold table), and M is a fixed safety margin (in dB). The number of 3-dB ADR adjustment steps is

$$N = \left\lfloor \frac{\Delta}{3} \right\rfloor \tag{11}$$

and ADR then updates the transmission parameters to obtain the next configuration (SF_{t+1}, P_{t+1}), where P_t is transmitting power (dBm) and t is the uplink index/time step. In the proposed approach, ADR is learned from data using a deep-learning LSTM: we form an input vector

$$\mathrm{x}_t = [\mathrm{SNR}_t, \mathrm{RSSI}_t, \mathrm{PER}_t] \tag{12}$$

Table 2
LoRaWAN symbol duration and ISI susceptibility (BW = 125 kHz).

SF	Symbol Duration (ms)	ISI Threshold (μs)	ISI Risk Level
SF7	1.024	10.24	High
SF8	2.048	20.48	High
SF9	4.096	40.96	Medium
SF10	8.192	81.92	Medium
SF11	16.384	163.84	Low
SF12	32.768	327.68	Very low

where SNR_t and RSSI_t are the measured link indicators at time t, and PER_t is packet loss. The LSTM uses the last L inputs $\mathrm{x}_{t-L+1},\ldots,\mathrm{x}_t$ to produce a hidden state h_t and predict the next ADR decision

$$\mathrm{h}_t = \mathrm{LSTM}(\mathrm{x}_t, \mathrm{h}_{t-1}) \tag{13}$$

and

$$\hat{\mathrm{y}}_{t+1} = W\mathrm{h}_t + b \tag{14}$$

where,

$$\hat{\mathrm{y}}_{t+1} = [\widehat{\mathrm{SF}}_{t+1}, \hat{P}_{t+1}] \tag{15}$$

W and b are the output-layer weight matrix and bias, and θ denotes all trainable network parameters (LSTM weights plus W, b). The LSTM is used by deep learning because θ is learned by minimizing a prediction loss

$$\mathscr{L} = \sum_t \|\hat{\mathrm{y}}_{t+1} - \mathrm{y}_{t+1}\|^2 \tag{16}$$

and updating with gradient descent

$$\theta \leftarrow \theta - \eta \nabla_\theta \mathscr{L} \tag{17}$$

where η is the learning rate and y_{t+1} is the target ADR setting.

3.4. Problem formulation

The proposed LSTM-DDPG Adaptive Modulation and Coding (LD-AMC) framework aims to jointly tune the LoRaWAN transmission parameters SF, CR, BW, and P_t to mitigate ISI while maintaining throughput and energy efficiency in dynamic maritime channels. Over-water links change rapidly because wave motion and sea-surface reflections create time-varying multipath, leading to large swings in delay spread that degrade LoRa demodulation performance [9]. Recent studies show that maritime multipath can introduce path-delay differences on the order of tens to hundreds of microseconds, which can severely disrupt chirp detection, particularly at low SFs [39]. These conditions motivate a learning-based, predictive adaptation mechanism that can adjust the physical-layer parameters proactively, before ISI becomes harmful. Fig. 1 shows how the weather conditions, signal reflections, and multiple transmission sources all contribute to signal fading and instability in maritime wireless communication systems.

3.4.1. Variables and state representation

LD-AMC models modulation and coding selection as a continuous state–action decision problem. At each time step t, the agent chooses an action.

$$a_t = [SF_t, CR_t, BW_t, P_t] \tag{18}$$

where SF_t, CRt, BWt, and P_t are the SF, CR, BW, and P_t selected at time t, respectively subject to LoRaWAN constraints: $SF_t \in \{7,8,9,10,11,12\}$, $CR_t \in \{4/5, 4/6, 4/7, 4/8\}$, $BW_t \in \{125, 250, 500\}$ kHz, and $\mathrm{P}_{min} \le \mathrm{P}_t \le \mathrm{P}_{max}$. These parameters jointly determine airtime, link budget, spectral utilization, and ISI susceptibility.

At each decision time, the environment provides a state vector.

$$s_t = \{RSSI_t, SNR_t, PER_t, \tau_{rms,t}, H_{s,t}, v_{ship,t}\} \tag{19}$$

where $RSSI_t$ and SNR_t represent link quality, PER_t captures recent decoding performance, $\tau_{rms,t}$ is the current RMS delay spread, $H_{s,t}$ denotes sea-state/wave height, and $v_{ship,t}$ is vessel speed. The prediction of delay spread provides ISI-awareness beyond conventional ADR methods, aligning with recent findings that delay-spread prediction significantly improves LoRaWAN reliability in mobile and multipath conditions [40].

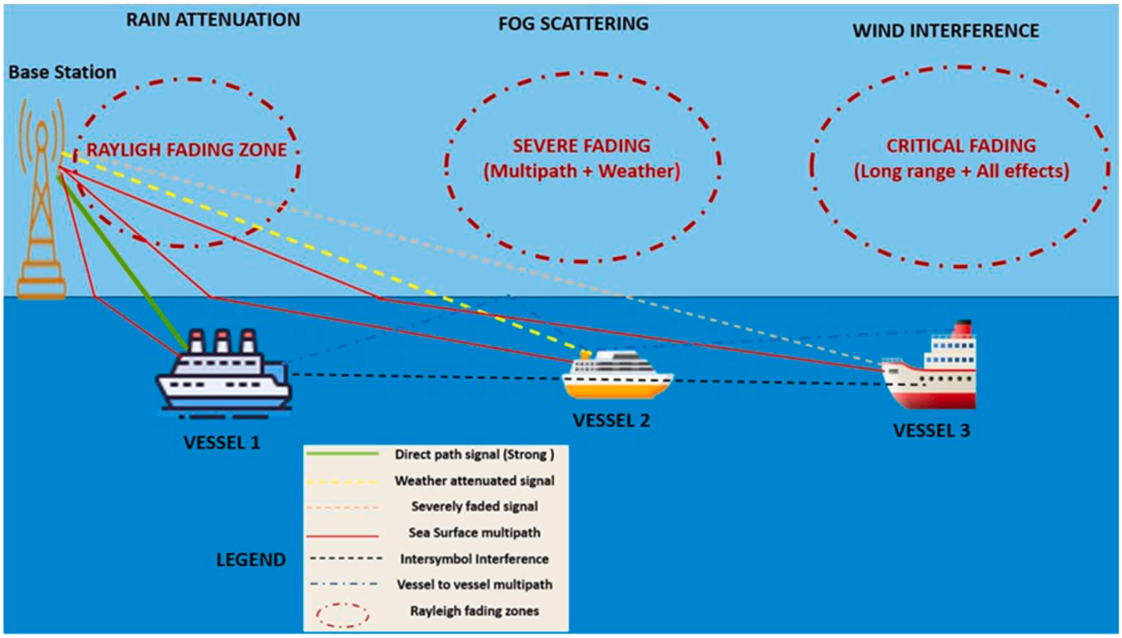

Fig. 1. Maritime channel impairments, including ISI.

3.4.2. *Learning objective*

The objective of LD-AMC is to learn a policy, (20) that maximizes long-term performance.

$$a_t = \pi_\theta(s_t) \tag{20}$$

where π_θ is the actor network parameterized by θ.

The expected discounted return (21) is

$$J(\theta) = \mathbb{E}\left[\sum_{k=0}^{\infty} \gamma^k r_{t+k}|_{\pi_\theta}\right] \tag{21}$$

where γ is the discount factor and r_t is the reward at time t.

To anticipate fast channel variations, LD-AMC employs an LSTM predictor trained on past observations to estimate short-term channel evolution (14):

$$\widehat{c}_{t+1} = f_{LSTM}(c_{t-W+1}, ...c_t) \tag{22}$$

where $\mathbf{c}_t$ is the vector of observed channel metrics at time t such as SNR, RSSI, and τ_{rms} while W is the window size. The enhanced state (23), allows the DDPG controller to make decisions based on predicted ISI conditions, consistent with recent reinforcement learning designs that incorporate channel forecasting for LPWAN optimization.

$$\widetilde{s}_t = [s_t, \widehat{c}_{t+1}] \tag{23}$$

3.4.3. *Reward formulation*

The reward function (24) balances reliability, throughput, energy cost, and ISI avoidance. At each time step,

$$r_t = w_1 PDR_t + w_2 T_t^{norm} - w_3 E_t^{norm} - w_4 I_t^{norm} \tag{24}$$

where $PDR_t$is the packet delivery ratio, T_t^{norm} is normalized throughput, E_t^{norm} is normalized energy per packet, I_t^{norm} is a normalized ISI severity metric, and w_3,..,w_4 are non-negative weighting factors (with $w_3, w_4 > 0$ so that higher energy use and higher ISI reduce the reward).

In summary, LD-AMC uses LSTM-based channel prediction and DDPG continuous control to select SF, CR, BW, and P_t within LoRaWAN constraints, thereby anticipating harmful ISI events and reducing packet losses due to maritime multipath [41].

4. Proposed LD-AMC framework

The proposed LD-AMC framework, as shown in Fig. 2, is designed to reduce ISI and enhance both link reliability and energy efficiency in maritime LoRaWAN deployments. In these environments, radio links are heavily affected by sea-surface reflections, wave-driven multipath, and moving platforms, which together cause fast changes in delay spread and fading conditions where conventional ADR often breaks down [9]. LD-AMC tackles these limitations by combining predictive learning with a reinforcement learning controller, allowing LoRaWAN nodes to anticipate harmful channel variations and adjust physical-layer parameters in advance, before ISI degrades performance.

4.1. *Framework overview*

LD-AMC is an adaptive closed-loop system consisting of three key components: ISI -aware feature extraction unit extracts the real-time link characteristics such as RSSI, SNR, PER and delay-spread parameters from the receiver; a predictive component based on LSTM predicts the future SNR, PER and delay spread using the historical data; finally, the AMC control block based on DDPG uses the combination of the current and future (predicted) channel state information and selects the appropriate PHY parameter setting SF, CR, BW, and P_t. The combined capability of the three modules of LD-AMC enables it to proactively modify LoRaWAN parameters and maintain stable communication in the rapidly changing conditions of the marine environment.

4.2. *ISI-aware feature extraction*

The first step in LD-AMC is to extract features that describe the channel's behaviour under ISI. In maritime links, multipath changes with wave motion, sea-surface roughness, vessel movement, and grazing angle, often creating delay spreads that low SFs cannot tolerate. Because standard ADR metrics like RSSI and SNR do not capture this, LD-AMC augments them with PER, estimated delay spread $\tau_{rsm,t}$, sea-state index $H_{s,t}$, vessel speed $v_{ship,t}$ (for Doppler), and, when available, a simple measure of multipath richness. Together, these quantities form the state vector. $\mathbf{s}_t$ fed to the LSTM predictor and DDPG controller, ensuring that modulation and coding choices are driven directly by ISI severity, in line with recent ISI-aware LoRaWAN optimization studies.

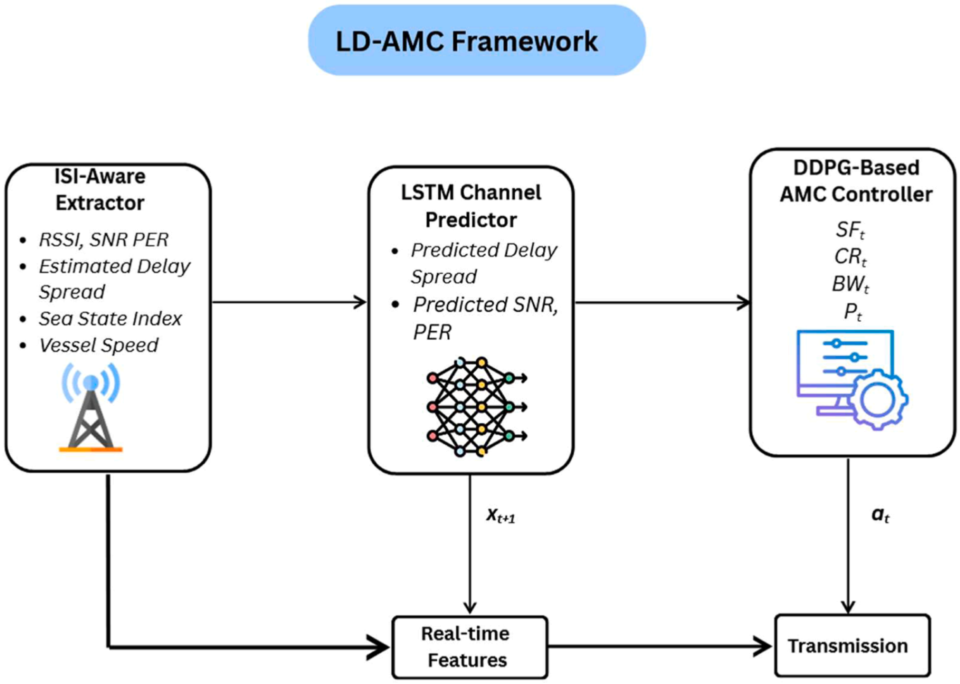

Fig. 2. LD-AMC framework with ISI-aware feature extraction, LSTM channel prediction, and DDPG-based AMC control for adaptive LoRaWAN transmission.

4.3. LSTM-based channel prediction

Maritime channels have a mix of structure and randomness: slow trends driven by wave patterns and fast fluctuations caused by local surface changes. LSTM networks are well-suited to this kind of time-dependent behaviour, and recent work has shown that they can reliably predict LPWAN and maritime channel conditions. In LD-AMC, the LSTM takes a sliding window of recent states (25),

$$\mathrm{X_t} = [\mathrm{s}_{t-W+1}, \ldots\ldots\mathrm{s_t}] \tag{25}$$

and maps it to a prediction of the next-step channel metrics (26),

$$\widehat{\mathrm{y}}_{t+1} = \mathrm{f_{LSTM}}(\mathrm{X_t}) \tag{26}$$

The predicted channel metrics $\widehat{\mathbf{y}}_{t+1}$ are then concatenated with the current observation $\mathbf{x}_t$ to form the enhanced state $\mathbf{s}_t$, allowing the DDPG agent to anticipate short-term channel evolution when selecting the adaptive modulation and coding action.

4.4. DDPG-based AMC controller

The DDPG-based AMC controller is the “brain” of LD-AMC. It continuously adjusts LoRaWAN parameters SF, CR, BW, and $\mathrm{P_t}$ rather than relying on coarse, rule-based ADR updates. The controller sees an

Algorithm 1
LD-AMC high-level adaptive modulation and coding procedure.

Input:
Maritime LoRaWAN environment E; discount factor γ; weights $w_1, \ldots, w_4$;
LSTM window size; replay buffer size.
Output:
Optimized LD-AMC policy π^* for selecting $[SF, CR, BW, P_t]$.
Begin
Initialize LSTM predictor, actor π, critic, target networks, and replay buffer D.
For each training episode **do**
Reset environment E; observe initial state x_0; initialize window W_0.
For each time step t in episode **do**
Predict short-term channel: $\widehat{x}_{t+1} \leftarrow \mathrm{LSTM}(W_t)$.
Form enhanced state: $s_t = [x_t, \widehat{x}_{t+1}]$.
Select action: $a_t = \pi(s_t) = [SF_t, CR_t, BW_t, P_t]$.
Apply a_t to LoRaWAN PHY/MAC.
Observe x_{t+1}; compute $PDR_t, T_t^{norm}, E_t^{norm}, I_t^{norm}$.
Compute reward:
$r_t = w_1 PDR_t + w_2 T_t^{norm} - w_3 E_t^{norm} - w_4 I_t^{norm}$.
Update window W_{t+1} and predict $\widehat{x}_{t+2} \leftarrow \mathrm{LSTM}(W_{t+1})$.
Form next enhanced state: $s_{t+1} = [x_{t+1}, \widehat{x}_{t+2}]$.
Store (s_t, a_t, r_t, s_{t+1}) in $\mathscr{D}$.
Sample minibatch from $\mathscr{D}$; update critic and actor (DDPG).
Soft-update target networks: $\bar{\theta} \leftarrow \tau\theta + (1-\tau)\bar{\theta}$, $\bar{\psi} \leftarrow \tau\psi + (1-\tau)\bar{\psi}$.
End For
End For
Return optimized policy π^*.
End Algorithm

enhanced state that combines live measurements with LSTM predictions, enabling it to react not only to the current channel but also to expected increases in delay spread and ISI. Using an actor–critic structure, it learns a policy that balances reliability, throughput, energy use, and ISI mitigation. In this way, the DDPG controller enables LD-AMC to achieve more stable maritime links, with higher packet delivery rates and fewer ISI-related errors than conventional ADR schemes.

Algorithm 1 summarizes the LD-AMC training loop. At each time step, recent link measurements are fed into an LSTM to predict short-term channel conditions, which are combined with the current observation to form an enhanced state for the DDPG agent. The actor then selects LoRaWAN parameters $[SF, CR, BW, P_t]$, and the resulting reward balancing PDR, normalized throughput, energy consumption, and ISI severity is used to update the actor–critic and LSTM networks toward an ISI-aware, energy-efficient adaptation policy.

4.5. Integration of LSTM prediction with DDPG control

LD-AMC operates under partial observability because instantaneous measurements (e.g., recent link-quality indicators and ACK outcomes) do not fully capture the evolving ISI conditions driven by sea-surface dynamics. The LSTM reduces this uncertainty by extracting a temporal representation from a sliding window of observations and predicting near-future channel/ISI behaviour. Let o_t denote the observation vector at decision time t and W the history length. The LSTM maps $\{o_{t-W+1}, \ldots, o_t\}$ to a predicted feature vector $\widehat{z}_{t+1}$:

$$\widehat{z}_{t+1} = f_{LSTM}\left(o_{t-W+1:t}\right) \tag{27}$$

The DDPG state is then formed by augmenting the current observation with the predicted features,

$$s_t = [o_t, \widehat{z}_{t+1}] \tag{28}$$

and the actor selects the LD-AMC action a_t (mapped to LoRaWAN PHY parameters) as in (20).

The critic evaluates the long-term value of the selected action under the predicted dynamics, enabling proactive adaptation rather than purely reactive parameter changes.

Effect of prediction errors: Let z_{t+1} be the true channel/ISI feature and $e_t = z_{t+1} - \widehat{z}_{t+1}$ the prediction error. The policy, therefore, acts in an approximate state $\widetilde{s}_t = [o_t, \widehat{z}_{t+1}]$. In LD-AMC, robustness to prediction errors is improved by training across diverse channel realizations and by replay-based learning, which exposes the agent to a wide range of prediction qualities. In addition, the reward design can discourage excessive parameter toggling, which helps maintain stable adaptations when prediction uncertainty increases. This explicitly explains how LSTM prediction and DDPG control synergize to mitigate ISI and stabilize PHY adaptation in time-varying maritime conditions.

4.6. Computational complexity and real-time feasibility

LD-AMC may appear computationally heavy because it combines an LSTM predictor with a DDPG controller; however, training is done offline, and the IoT node performs only online inference during operation. At run time, the device executes a forward pass through the LSTM to predict short-term channel/ISI behaviour and a forward pass through the actor network to select PHY adaptation parameters. Since these computations are mainly multiply-accumulate operations and are triggered at the adaptation timescale (typically once per packet/decision interval), they align well with LoRaWAN's sporadic transmissions and duty-cycle limits. Deployment cost can be further reduced using smaller models (guided by sensitivity analysis), quantization/pruning and when feasible, gateway/edge-assisted inference where the node sends lightweight features and receives configuration recommendations.

4.7. Training details and stability

During training, LD-AMC balances exploration and exploitation by adding correlated exploration noise to the actor output, enabling efficient exploration in continuous action spaces. Specifically, the executed action is

$$a_t = \pi_\theta(s_t) + \epsilon_t \tag{29}$$

where $\pi_\theta(\cdot)$ is the actor policy and $\epsilon_t$follows an Ornstein–Uhlenbeck (OU) process:

$$\epsilon_{t+1} = \epsilon_t + \theta(\mu - \epsilon_t)\Delta t + \sigma\sqrt{\Delta t}\, w_t \tag{30}$$

with $w_t \sim \mathcal{N}(0,1)$. In our implementation, $\mu = 0$, $\theta = 0.15$, and $\sigma = 0.2$. Each transition (s_t, a_t, r_t, s_{t+1}) is stored in an experience replay buffer $\mathscr{D}$, and mini-batches are sampled from $\mathscr{D}$ to reduce temporal correlation and improve sample efficiency. To stabilize learning, we employ target networks for both actor and critic, $\pi_{\bar{\theta}}$ and $Q_{\bar{\psi}}$, updated using soft updates:

$$\bar{\theta} \leftarrow \tau\theta + (1-\tau)\bar{\theta} \tag{31}$$

$$\bar{\psi} \leftarrow \tau\psi + (1-\tau)\bar{\psi} \tag{32}$$

where $\tau \ll 1$. The critic is trained by minimizing the temporal-difference loss

$$\mathscr{L}(\psi) = \mathbb{E}_{(s,a,r,s')\sim\mathscr{D}}\left[(Q_\psi(s,a) - y)^2\right] \tag{33}$$

with target

$$y = r + \gamma Q_{\bar{\psi}}\left(s', \pi_{\bar{\theta}}(s')\right) \tag{34}$$

where γ is the discount factor, these mechanisms (OU exploration noise, replay learning, and target networks) improve convergence and reduce unstable oscillations when training under time-varying maritime channel dynamics.

4.8. Hyperparameter selection and reproducibility

The LSTM and DDPG hyperparameters were selected to balance learning stability, generalization, and deployment feasibility. The LSTM hidden size controls temporal representation capacity; excessively small values underfit fast maritime variations, whereas excessively large values increase computation and may overfit simulation dynamics. The actor/critic learning rates were chosen to maintain stable critic convergence and avoid policy collapse; the target update rate τ and replay buffer size were selected following common DDPG stabilization practice and verified empirically for stable learning curves. To support reproducibility, we report the complete training configuration (such as network sizes, optimizers, learning rates, replay buffer size, batch size, exploration noise schedule, discount factor, and target update rate) and include random seeds and averaging across multiple runs.

5. Simulation setup

To evaluate the proposed LD-AMC framework under realistic maritime variability, we developed a MATLAB/Simulink-based system-level simulator that combines (i) a LoRaWAN PHY configuration (SF/CR/BW and P_t), (ii) a two-ray maritime channel with time-varying reflection and delay spread, and (iii) a packet-level Media Access Control (MAC) abstraction to compute delivery outcomes and energy per delivered packet. Simulink is used to leverage validated signal-processing blocks for fading/noise and to ensure consistent, repeatable link evaluation across the tested scenarios.

5.1. Maritime scenario and mobility model

The simulations assume a coastal/offshore maritime environment with wide-open water and strong over-sea multipath, suitable for analyzing ISI in LoRaWAN links. Vessels follow AIS-derived mobility traces that capture realistic speeds and heading changes, and a set of fixed LoRaWAN gateways distributed along the coastline provides long-range ship-to-shore connectivity. This setup captures both slow and fast channel variations, so Doppler shifts, delay-spread changes, and multipath effects are realistically represented.

5.2. LoRaWAN PHY and MAC configuration

The simulations use standard LoRaWAN regional settings with a full LoRa physical layer. Carrier frequency of 868 MHz, BWs of 125, 250 and 500 kHz are considered, with SF7-SF12 and CRs 4/5, 4/6, 4/7 and 4/8. $\mathrm{P_t}$ varies from 2 to 14 dBm, and payload sizes range from 20 to 100 bytes to reflect typical maritime telemetry traffic.

The MAC layer is modelled as a pure ALOHA uplink with a 1 % duty cycle. Retransmissions are allowed for the baseline schemes but not for LD-AMC, since LD-AMC adjusts the PHY parameters on its own. Standard ADR is disabled except when used as an explicit comparison baseline, so that any performance gains can be clearly attributed to LD-AMC.

5.3. Baseline algorithms for comparison

Three baselines are used against LD-AMC. The first is standard LoRaWAN ADR, which updates SF and $\mathrm{P_t}$ only from averaged SNR and has no prediction or ISI awareness. The second is a maritime-tuned ADR with adjusted SNR thresholds, but it is still reactive and blind to delay spread. The third is a simple heuristic AMC scheme that picks SF, CR, BW and $\mathrm{P_t}$ using fixed RSSI/SNR rules, without any learning or channel prediction. These baselines reflect common practice in real deployments, while LD-AMC adds both prediction and explicit ISI awareness.

5.4. Evaluation metrics

Performance was evaluated using a small set of clear metrics. Reliability was measured using the PDR, the fraction of packets that arrived correctly. *ISI impact* was assessed through an error measure based on the overlap ratio $\Delta\tau/T_s$. *Energy efficiency* was captured by the average energy spent per successfully delivered packet, combining time-on-air and $\mathrm{P_t}$. *Throughput* was defined as the useful application data delivered per unit time, and spectral efficiency as the delivered bits per hertz of bandwidth. Finally, the *average SF* used by each scheme was tracked to show whether it tended to choose safer but slower settings (high SF) or faster, more ISI-sensitive ones (low SF).

Additional IoT service metrics: In addition to PDR/PER and energy efficiency, we also assess delivery latency and connection stability, which are key service-level indicators in IoT deployments. For LoRaWAN uplinks, delivery latency is largely determined by the selected PHY configuration through the packet ToA and any retransmissions; we therefore quantify average delivery latency as

$$\tau_{\mathrm{del}} = \mathbb{E}\left[\mathrm{ToA}(\mathrm{a_t})\cdot \mathrm{N_{tx}}\right] \tag{35}$$

where ToA (a_t) is the time-on-air under action a_t and N_{tx} is the number of transmission attempts until success (bounded by the retry limit). We quantify connection stability as the probability of sustaining a target delivery reliability over a service window T_s:

$$\mathscr{S} = \Pr\left(\mathrm{PDR}_{\mathrm{T_s}}\rho_{\min}\right) \tag{36}$$

where $\rho_{\min}$ denotes the minimum acceptable reliability for the application. These definitions allow latency and reliability continuity to be discussed consistently with the proposed adaptation strategy.

5.5. Simulation data generation methodology

All results in Section 6 come from a MATLAB/Simulink-based system-level simulator built to mimic LoRaWAN operation in a dynamic maritime setting. The simulator jointly models the over-sea radio channel, the LoRa physical layer, ISI effects, and the behaviour of both the baseline schemes and the proposed LD-AMC algorithm. The vessel–gateway channel is generated using a two-ray maritime model consistent with ITU-R P.1546–6 and ITU-R P.1411–10, where the direct and sea-reflected paths depend on vessel and gateway heights, sea-surface geometry, and wave-height statistics taken from NOAA buoy data. At each time step, the simulator computes the amplitudes of the direct and reflected paths, their delay difference and phase, and from these derives the power delay profile and RMS delay spread. Vessel positions and motion follow AIS-based mobility traces, providing realistic time-varying geometry and Doppler behaviour. A simplified LoRa PHY is implemented using standard symbol duration, time-on-air, and chirp detection thresholds, allowing instantaneous SNR and delay spread to be mapped to symbol and packet error rates. Following works such as Demeslay et al. (2021) [15], ISI severity is evaluated as a function of the normalized delay ratio $\Delta\tau/T_s$, so packet reliability can be computed at each transmission.

Each adaptation strategy (standard ADR, maritime-tuned ADR, heuristic AMC, and LD-AMC) runs inside this loop. Standard ADR uses only RSSI and SNR trends; the maritime ADR version applies more conservative rules; the heuristic AMC scheme uses fixed SNR-based rules to pick SF, CR, BW, and $\mathrm{P_t}$. LD-AMC instead uses an LSTM model to predict short-term channel conditions (SNR, RSSI, delay spread) and a DDPG agent to select $(\mathrm{SF},\ \mathrm{CR},\ \mathrm{BW},\ \mathrm{P})$ that maximize a multi-objective reward combining delivery success, energy cost, ISI risk, and throughput. At every step, the chosen parameters are applied to the PHY model, and the simulator logs whether the packet was received, the energy spent, the achieved throughput, spectral efficiency, and the SF used. Energy is computed from transmit current, supply voltage, and time-on-air (including retransmissions where applicable); throughput is measured as useful bits delivered per unit time, and spectral efficiency is throughput divided by active bandwidth.

Each configuration is run over a 72-hour mission and repeated 50 times in Monte Carlo trials with independent noise, mobility, and wave realizations. Final metrics, PDR, ISI-induced error rate, energy per successful packet, throughput, and spectral efficiency are obtained by averaging over all runs. A block diagram summarizing this pipeline from channel synthesis through LoRa PHY and ISI evaluation to algorithm decisions and metric computation is shown in Fig. 3.

5.6. Hyperparameter settings

Table 3 lists the main LSTM predictor and DDPG controller hyperparameters used in the simulations. These values were kept fixed across all sea-state scenarios.

Simulation-based validation statement: This research evaluates the performance of LD-AMC using MATLAB/Simulink-generated data within the context of a maritime communication channel model that captures the primary reflection-driven ISI characteristics of the environment. No field measurements or sea-trial experiments were conducted as part of this work. Consequently, the reported results demonstrate the potential performance gains under controlled and reproducible conditions. We consider real-world validation accounting for device hardware non-idealities, protocol timing constraints, external interference, and site-specific maritime propagation variability as an essential next step and describe it explicitly in the limitations and future Work section.

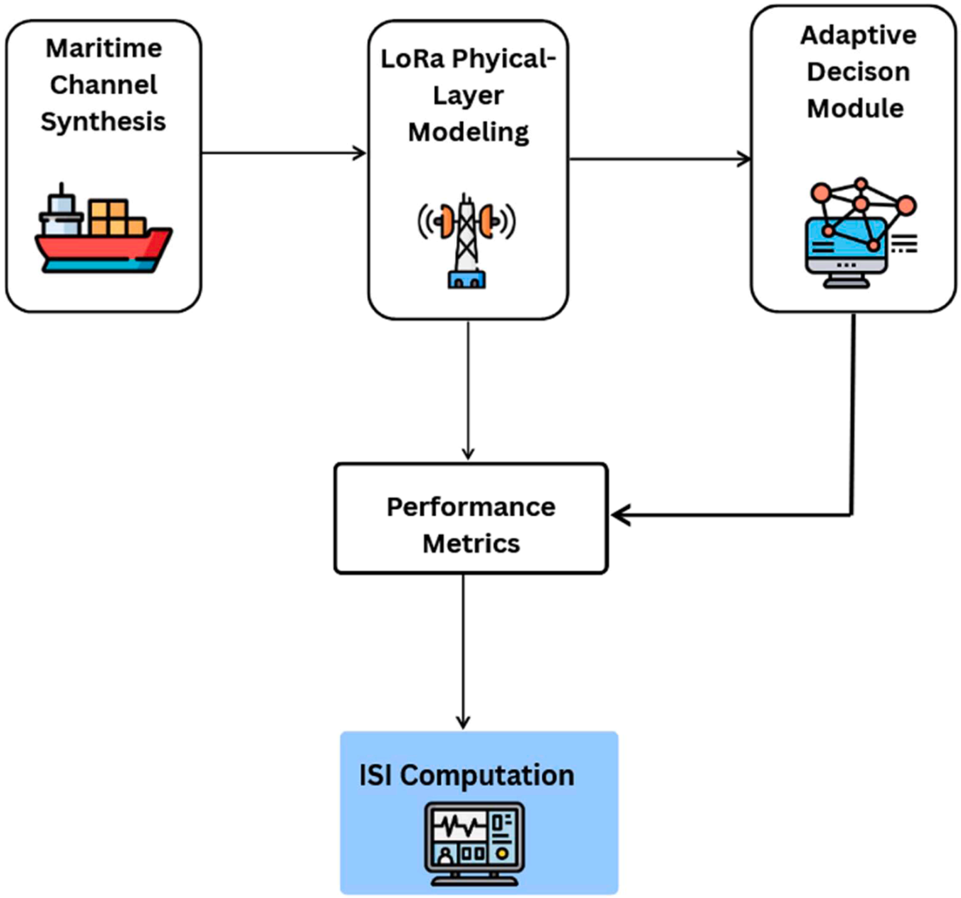

Fig. 3. Simulation pipeline for LD-AMC evaluation, showing maritime channel synthesis, LoRa physical-layer modelling, ISI computation, adaptive decision module (ADR, AMC, or LD-AMC), and final performance metric aggregation.

Table 3
Hyperparameter settings for the LSTM predictor and DDPG controller.

Component	Hyperparameter	Value
DDPG	Discount factor (γ)	0.99
DDPG	Target soft update (τ)	0.005
DDPG	Actor learning rate	1e-4 (Adam)
DDPG	Critic learning rate	1e-3 (Adam)
DDPG	Replay buffer size	1000,000
DDPG	Mini-batch size	256
DDPG	Exploration noise	Ornstein–Uhlenbeck; σ=0.2, θ=0.15
DDPG	Training episodes / steps	500 episodes; 1000 steps/episode
Reward	Weights (λ_PDR, λ_T, λ_E, λ_ISI)	(0.4, 0.3, 0.2, 0.1)
LSTM	Input window length (W)	10
LSTM	Hidden units / layers	32 units; 1 layer
LSTM	Optimizer / learning rate	Adam; 1e-3

6. Results and discussion

This section reports how the LD-AMC framework performs under dynamic maritime conditions. The results show clear gains in link reliability, ISI mitigation, and energy efficiency when compared with traditional ADR-based schemes. All metrics are obtained from 72-hour simulations that include realistic vessel movement, changing sea states, and time-varying multipath.

For convenience, Table 4 summarizes the key relative gains reported in Figs. 4–8 (all averaged over 50 Monte Carlo runs of the 72-hour mission).

Table 4
Summary of key performance gains of LD-AMC (relative to baselines).

Metric	LD-AMC vs. baseline	Gain (range / max)	Figure
(PDR)	Standard ADR	Up to +47 %	Fig. 4
ISI-induced symbol error rate	Standard ADR	Up to 58 % reduction	Fig. 5
Energy per successful packet	Standard ADR	≈ 32 % reduction	Fig. 6
Throughput	Standard ADR	+22 % to +34 %	Fig. 7
Throughput	Maritime-tuned ADR	+12 % to +18 %	Fig. 7
Spectral efficiency	ADR	+15 % to +22 %	Fig. 8

6.1. PDR

As illustrated in Fig. 4, LD-AMC demonstrates consistent improvement in PDR performance with increasing sea surface roughness, accompanied by a corresponding increase in multipath effects and ISI delay spread. In contrast to the substantial decline in reliability observed for both standard ADR and heuristic AMC under these conditions, LD-AMC shows superior PDR performance at all levels of sea state; specifically, LD-AMC provides an average of 47 % better performance than standard ADR in the high sea states, due to LD-AMC's proactive adjustments to SF, CR, BW, and transmit power based upon ISI performance prediction.

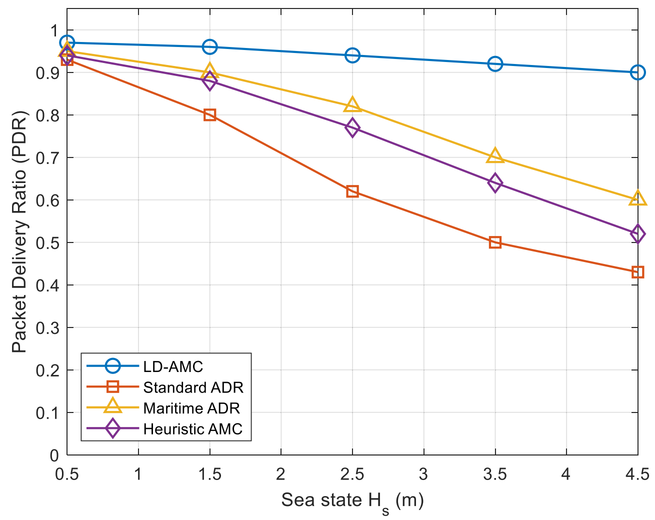

Fig. 4. PDR versus sea state H_s. LD-AMC achieves significantly higher PDR across all sea conditions through proactive ISI mitigation enabled by predictive channel modelling and continuous AMC control.

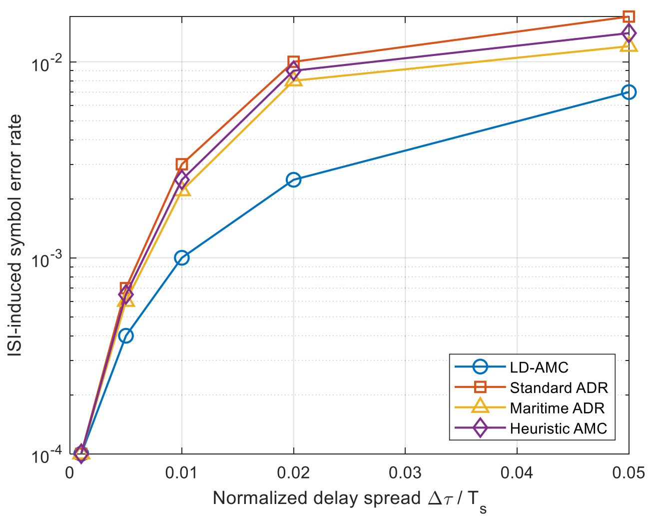

Fig. 5. ISI-induced symbol error rate versus normalized delay spread $\Delta\tau / T_s$. LD-AMC outperforms all baseline methods by anticipating ISI-prone conditions and selecting more resilient transmission configurations.

6.2. ISI-induced error rate

As shown in Fig. 5, the ISI-induced symbol error rate rises sharply as the normalized delay spread increases with respect to sea-state based on arrival time and strength of reflected signal components. The LD-AMC method significantly reduces these ISI-based errors; specifically, it achieves a 58 % improvement over standard ADR performance. These improvements are achieved by selecting ISI-sensitive parameters based on the LSTM predictor's output when it detects increased delay spread.

6.3. Energy consumption per successful packet

As demonstrated in Fig. 6, as the sea state worsens, the energy usage of all the baseline schemes will increase due to increased retransmissions and longer time in the air when using a larger SF. Using predictive channel knowledge to minimize retransmits and avoid unnecessary high-power and/or high-SF transmissions, LD-AMC reduces energy usage by about 32 % compared to ADR.

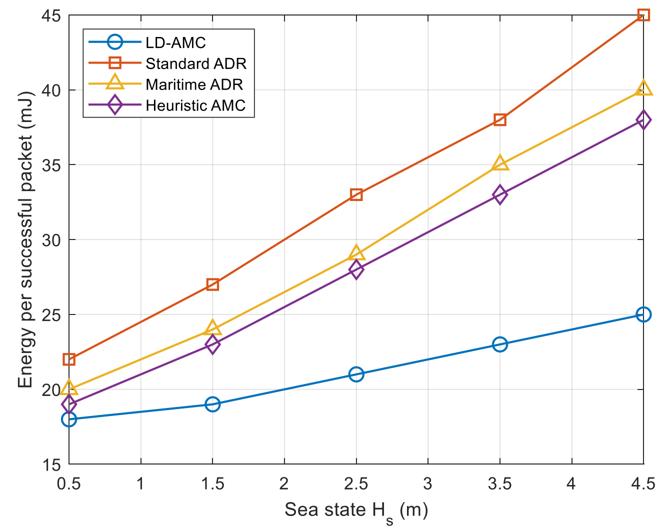

Fig. 6. Average energy consumption per successfully delivered packet across sea states. LD-AMC offers the lowest energy cost through its predictive, ISI-aware control policy, which reduces retransmissions and avoids inefficient configurations.

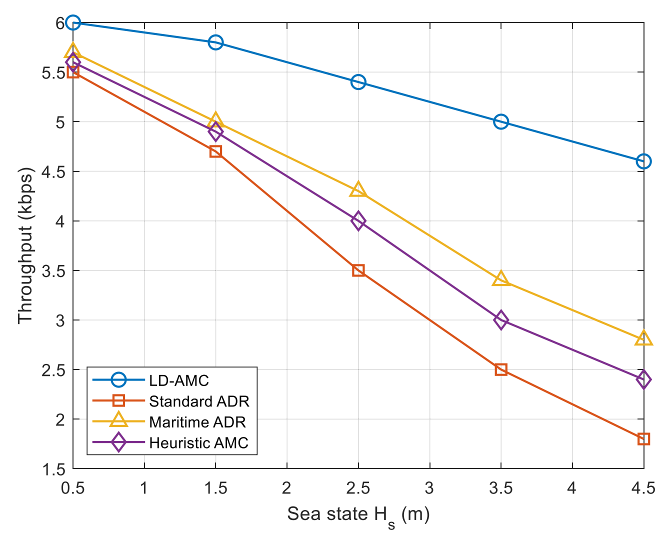

Fig. 7. Application-layer throughput versus sea state H_s.

6.4. Throughput performance

Throughput is strongly dependent on the chosen SF and BW, as well as the packet success rate. Although LD-AMC occasionally selects higher SFs to mitigate ISI, the overall throughput is consistently higher than that of baseline methods due to fewer packet losses.

Across all sea states, LD-AMC yields a 22–34 % increase in average throughput over ADR, and a 12–18 % gain over maritime-tuned ADR as shown in Fig. 7. The heuristic AMC scheme shows moderate improvements in calm seas but fails to maintain stability under fast-changing multipath conditions. LD-AMC uses throughput stability to adjust BW and CRs based on predictions of channel behaviour rather than simply reacting to current instantaneous SNR.

6.5. Spectral efficiency and parameter utilization

The spectral efficiency results in Fig. 8 highlight how LD-AMC balances aggressive and conservative parameter choices. While ADR frequently defaults to higher SFs in uncertain conditions, LD-AMC

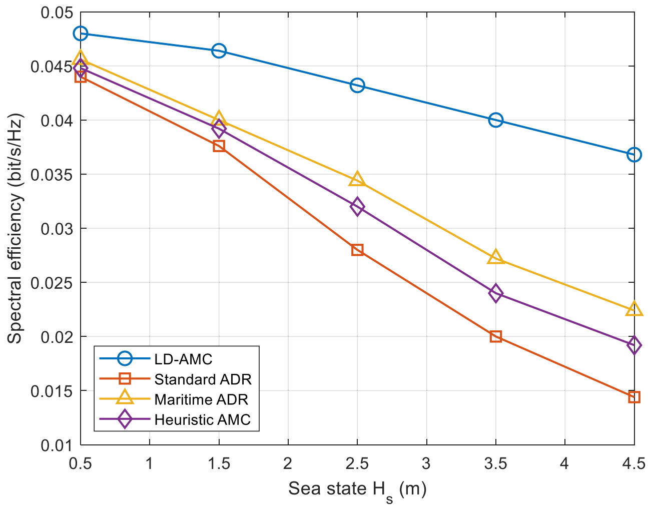

Fig. 8. Spectral efficiency versus sea state H_s for LD-AMC, standard ADR, maritime-tuned ADR, and heuristic AMC. LD-AMC maintains higher spectral efficiency under dynamic maritime conditions by combining predictive channel modelling with proactive AMC decisions.

selectively applies them only when rising delay spread is predicted. This selective behavior increases spectral efficiency by 15–22 % compared to ADR.

An analysis of parameter utilization shows that LD-AMC maintains an average SF of 9.1, compared to 10.7 for ADR, reflecting LD-AMC's ability to operate efficiently under conditions where ADR would otherwise fall back to low data rates.

6.6. Spreading factor utilization distribution

Fig. 9 compares how different schemes allocate spreading factors across the network. Standard ADR sticks with high SFs (SF11–12) most of the time, which lowers spectral efficiency and wastes airtime. LD-AMC demonstrates adaptive efficiency by selecting lower SFs under favorable channel conditions and only increases when ISI increases. This behavior explains why LD-AMC achieves superior throughput, energy performance, and spectral efficiency.

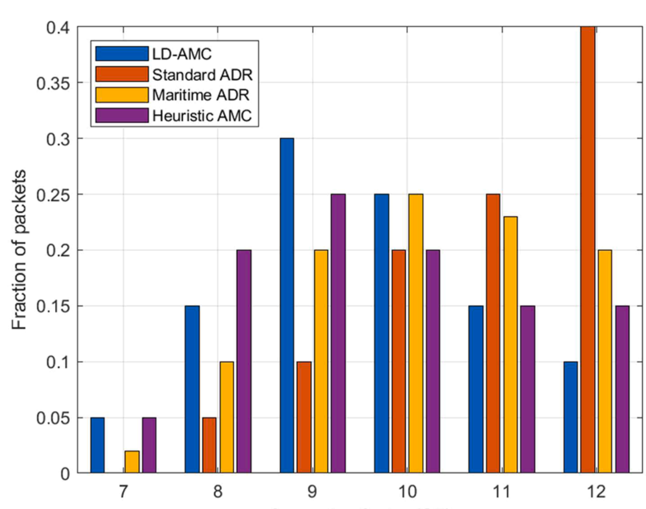

Fig. 9. Distribution of packets over SFs (SF7-SF12) for LD-AMC and the three baseline schemes during the 72-hour maritime simulation.

6.7. Sensitivity analysis of key hyperparameters

We evaluate the sensitivity of LD-AMC to key hyperparameters that influence performance and reproducibility: (i) LSTM window length W, (ii) LSTM hidden units h, (iii) actor/critic learning rates (α_π, α_Q) and (iv) reward weights. Each parameter is varied while holding others fixed, and results are reported in terms of PER/PDR, throughput, and energy per successful packet. The analysis confirms that LD-AMC performance is robust within a practical range and motivates the default configuration used in subsequent experiments. In particular, we vary the reward weights in (24) to quantify the trade-off between reliability, throughput, energy cost, and ISI mitigation.

6.8. Discussion of results

The results show that LD-AMC gives clear benefits over standard ADR and the heuristic AMC schemes in a changing maritime channel. The main reason is that LD-AMC has some advanced knowledge of how delay spread is likely to change. With the LSTM predictor, the controller can detect when the delay spread is increasing and adjust SF, CR, BW, and P_t before ISI becomes severe. Standard ADR, in contrast, only looks at current SNR and tends to react after PDR has already dropped. This explains why LD-AMC keeps a smoother PDR curve and a much lower ISI-induced symbol error rate across all sea states.

Another important point is how LD-AMC manages the trade-off between reliability and efficiency. When conditions are uncertain, ADR often uses high SF values for extended periods, which increases airtime, energy use, and collision risk. LD-AMC only moves to these robust settings when the predicted delay spread exceeds a risk threshold, and it returns to lower SF and wider BW when the channel improves. This behavior leads to higher spectral efficiency and lower energy per successful packet, as seen in the previous subsections.

DDPG's continuous action space prevents abrupt parameter transitions that would occur with discrete policy methods. LD-AMC can adjust BW and P_t in finer increments instead of large discrete jumps, which reduces oscillations and improves adaptation stability. Even when the LSTM prediction is not exact, the critic uses the long-term reward to smooth out these errors, so the learned policy stays robust.

Taken together, the results suggest that LD-AMC attacks the main cause of performance loss in maritime LoRaWAN, unpredictable ISI from sea reflections and moving platforms, rather than only reacting to changes in RSSI or SNR. The combination of prediction and adaptive control gives a practical way to keep long-range maritime IoT links reliable and energy-efficient.

7. Conclusion and future work

This work has presented LD-AMC, an adaptive modulation and coding framework for LoRaWAN in maritime environments. LD-AMC combines an LSTM-based channel predictor with a DDPG controller that adjusts SF, CR, BW and P_t in real time. The key idea is to bring delay-spread estimation and short-term channel prediction into the adaptation loop, so that the system can respond to ISI caused by sea-surface reflections and vessel motion before it leads to major packet loss.

Simulation results based on a North Sea–type scenario and a time-varying two-ray model augmented with a delay-spread component show consistent gains. LD-AMC achieves up to 47 % higher PDR than standard ADR, reduces ISI-induced symbol errors by about 58 %, and cuts energy per successful packet by roughly 32 %. It also improves spectral efficiency and maintains a more stable throughput by using higher-rate configurations whenever the predicted channel state allows it. These results indicate that prediction-driven adaptation is well-suited to offshore IoT use cases such as buoy networks, coastal monitoring and autonomous ships.

A key limitation of this work is that the evaluation is entirely simulation-based and does not include real maritime measurements or sea trials. Although the adopted models capture dominant maritime mechanisms, such as reflection-driven excess delay variations and ISI effects, practical deployments may introduce additional factors, including hardware non-idealities, antenna placement effects, unmodeled interference/collisions, and weather-dependent attenuation.

There are several directions for future work. The current design assumes that training and decision logic are centred at the gateway. A natural extension is to develop a lighter, distributed version of LD-AMC that can run partly on end devices. Another method to achieve multi-agent coordination would be through multi-agent reinforcement learning techniques, whereby multiple nodes or vessels may make coordinated choices based on parameter values, potentially decreasing interference. Another potential solution is federated learning, where knowledge about channel behavior can be shared between deployments without sharing the actual data collected during those deployments; this could lead to better generalization across different sea states. Furthermore, this work will include embedded implementation profiling (memory, runtime, and energy) on representative LoRaWAN-class measurement-driven multipath and weather-dependent attenuation models (including sea spray/salt fog), and, finally, field trials and longer deployments at sea are needed to confirm the simulation results under real operating conditions.

Scalability considerations: While our evaluation focuses on a single link to isolate the ISI mitigation mechanism, LD-AMC can be extended to multi-vessel and multi-gateway deployments. A practical baseline is per-device-independent adaptation, where each device runs LD-AMC using its local observations and feedback, scaling linearly with the number of devices. In denser scenarios, gateway diversity and shared-spectrum contention introduce coupling between users; therefore, gateway-assisted coordination or multi-agent extensions may be considered to improve fairness and stability under collisions and duty-cycle constraints. These aspects, together with communication overhead and convergence under non-stationary multi-user dynamics, are identified as important directions for future work.

In summary, LD-AMC shows that combining channel prediction with adaptive control can significantly improve reliability, energy use and ISI resilience for maritime LoRaWAN links, and it provides a concrete step toward more intelligent offshore IoT communication systems.

CRediT authorship contribution statement

Martine Lyimo: Conceptualization, Formal analysis, Investigation, Methodology, Writing – original draft. **Bonny Mgawe:** Data curation, Software, Writing – review & editing. **Judith Leo:** Project administration, Supervision, Writing – review & editing. **Mussa Dida:** Formal analysis, Methodology, Validation, Writing – review & editing. **Kisangiri Michael:** Resources, Supervision, Writing – review & editing.

Declaration of competing interest

The authors declare that they have no known competing financial interests or personal relationships that could have appeared to influence the work reported in this paper.

Acknowledgements

The authors wish to acknowledge the support and constructive feedback from colleagues and the Nelson Mandela African Institution of Science and Technology during this research. This research did not receive any specific grant from funding agencies in the public, commercial, or not-for-profit sectors.

Data availability

The datasets generated and analyzed during this study are based on simulations. All simulation codes, configuration files, and results are available from the corresponding author upon reasonable request.

References

[1] J. Pinelo, A.D. Rocha, M. Arvana, J. Gonçalves, N. Cota, P. Silva, Unveiling LoRa's oceanic reach: assessing the coverage of the Azores LoRaWAN network from an island, Sensors 23 (17) (2023), https://doi.org/10.3390/s23177394. Sep.
[2] M.A.M. Almuhaya, W.A. Jabbar, N. Sulaiman, S. Abdulmalek, A Survey on LoRaWAN Technology: Recent Trends, Opportunities, Simulation Tools and Future Directions, MDPI, 2022, https://doi.org/10.3390/electronics11010164. Jan. 01.
[3] M. Lyimo, B. Mgawe, J. Leo, M. Dida, K. Michael, Adaptive antenna for Maritime LoRaWAN: a systematic review on performance, energy efficiency, and environmental resilience, Sensors 25 (19) (2025) 6110, https://doi.org/10.3390/s25196110. Oct.
[4] J. Cecílio, P.M. Ferreira, A. Casimiro, Evaluation of lora technology in flooding prevention scenarios, Sens. (Switz.) 20 (14) (2020) 1–24, https://doi.org/10.3390/s20144034. Jul.
[5] K. Anwar, T. Rahman, A. Zeb, I. Khan, M. Zareei, C. Vargas-Rosales, RM-ADR: resource management adaptive data rate for mobile application in LoRaWAN, Sensors 21 (23) (2021), https://doi.org/10.3390/s21237980. Dec.
[6] C.P. Davey, I. Shakeel, R.C. Deo, E. Sharma, S. Salcedo-Sanz, J. Soar, End-to-end learning of adaptive coded modulation schemes for resilient wireless communications, Appl. Soft Comput 159 (2024), https://doi.org/10.1016/j.asoc.2024.111672. Jul.
[7] M.A.A. Khan, H. Ma, A. Farhad, A. Mujeeb, I.K. Mirani, M. Hamza, When LoRa meets distributed machine learning to optimize the network connectivity for green and intelligent transportation system, Green Energy Intell. Transp. 3 (3) (2024), https://doi.org/10.1016/j.geits.2024.100204. Jun.
[8] C. Lehong, B. Isong, F. Lugayizi, and A.M. Abu-Mahfouz, "A survey of LoRaWAN adaptive data rate algorithms for possible optimization," 2020. doi: https://doi.org/10.1109/IMITEC50163.2020.9334144.
[9] Y. He, et al., A novel 3D non-stationary maritime wireless channel model, IEEE Trans. Commun. 70 (3) (2022) 2102–2116, https://doi.org/10.1109/TCOMM.2021.3134275. Mar.
[10] N. Cruz, et al., Extending LoRaWAN: mesh architecture and performance analysis for long-range IoT connectivity in maritime environments, Systems 13 (5) (2025), https://doi.org/10.3390/systems13050381. May.
[11] K. Anwar, et al., Improving the convergence period of adaptive data rate in a long range wide area network for the internet of things devices, Energ. (Basel) 14 (18) (2021), https://doi.org/10.3390/en14185614. Sep.
[12] A. Alwarafy, M. Abdallah, B.S. Ciftler, A. Al-Fuqaha, M. Hamdi, Deep Reinforcement Learning for Radio Resource Allocation and Management in Next Generation Heterogeneous Wireless Networks: A Survey, TechRxiv, 2021, https://doi.org/10.36227/techrxiv.14672643. May.
[13] F. Li, Y. Shui, J. Liang, K. Yang, J. Yu, Ship-to-ship maritime wireless channel modeling under various sea state conditions based on REL model, Front. Mar. Sci 10 (2023), https://doi.org/10.3389/fmars.2023.1134286.
[14] S. Pensieri, et al., Evaluating LoRaWAN connectivity in a marine scenario, J. Mar. Sci. Eng 9 (11) (2021), https://doi.org/10.3390/jmse9111218. Nov.
[15] C. Demeslay, P. Rostaing, and R. Gautier, "Theoretical performance of LoRa system in multi-path and interference channels," Jan. 2022, doi: 10.1109/JIOT.2021.3114439.
[16] L. Parri, S. Parrino, G. Peruzzi, A. Pozzebon, Low power wide area networks (LPWAN) at sea: performance analysis of offshore data transmission by means of LoRaWAN connectivity for marine monitoring applications, Sens. (Switz.) 19 (14) (2019), https://doi.org/10.3390/s19143239. Jul.
[17] R. Kufakunesu, G.P. Hancke, A.M. Abu-Mahfouz, A Survey on Adaptive Data Rate Optimization in Lorawan: Recent solutions and Major Challenges, MDPI AG, 2020, https://doi.org/10.3390/s20185044. Sep. 02.
[18] M.A. Lodhi, L. Wang, A. Farhad, ND-ADR: nondestructive adaptive data rate for LoRaWAN Internet of Things, Int. J. Commun. Syst. 35 (9) (2022), https://doi.org/10.1002/dac.5136. Jun.
[19] R. Carvalho, F. Al-Tam, N. Correia, Q-learning ADR agent for LoRaWAN optimization, in: Proceedings - 2021 IEEE International Conference on Industry 4.0, Artificial Intelligence, and Communications Technology, IAICT 2021, Institute of Electrical and Electronics Engineers Inc., 2021, pp. 104–108, https://doi.org/10.1109/IAICT52856.2021.9532518. Jul.
[20] S. Thenginthody Hassan, P. Chen, Y. Rong, K.Y. Chan, Underwater acoustic orthogonal frequency-division multiplexing communication using deep neural network-based receiver: river trial results, Sensors 24 (18) (2024), https://doi.org/10.3390/s24185995. Sep.
[21] M.H. Bagherian, Y.H. Tehrani, S.M. Atarodi, Enhancing LoRaWAN localization efficiency: leveraging machine learning and optimized parameter tuning for a 60% improvement, Meas. (L.) 242 (2025), https://doi.org/10.1016/j.measurement.2024.116064. Jan.
[22] L. Huang, Y. Wang, Q. Zhang, J. Han, W. Tan, Z. Tian, Machine learning for underwater acoustic communications, IEEE Wirel. Commun 29 (3) (2022) 102–108, https://doi.org/10.1109/MWC.2020.2000284. Jun.
[23] L. Acosta-Garcia, J. Aznar-Poveda, A.J. Garcia-Sanchez, J. Garcia-Haro, T. Fahringer, Dynamic transmission policy for enhancing LoRa network performance: a deep reinforcement learning approach, Internet Things (Neth.) 24 (2023), https://doi.org/10.1016/j.iot.2023.100974. Dec.

[24] D.H. Kim, J.Y. Pyun, AI-driven adaptive data rate for LoRaWAN location-based services, IEEe Access. 12 (2024) 168349–168359, https://doi.org/10.1109/ACCESS.2024.3494874.
[25] A. Farhad, J.Y. Pyun, AI-ERA: artificial intelligence-empowered resource allocation for LoRa-enabled IoT applications, IEEE Trans. Ind. Inf. 19 (12) (2023) 11640–11652, https://doi.org/10.1109/TII.2023.3248074. Dec.
[26] M. Wu, et al., RIS-assisted SATINs with RSMA and DRL: a trade-off between spectral, secrecy, and energy efficiency, IEEE Trans. Commun. 73 (11) (2025) 12380–12395, https://doi.org/10.1109/TCOMM.2025.3573454.
[27] M. Wu, et al., Federated learning driven covert communication in satellite terrestrial integrated networks: a privacy-preserving framework, IEEE J. Sel. Areas Commun. (2025), https://doi.org/10.1109/JSAC.2025.3637733.
[28] Z. Lin, M. Lin, T. De Cola, J.B. Wang, W.P. Zhu, J. Cheng, Supporting IoT with rate-splitting multiple access in satellite and Aerial-integrated networks, IEEe Internet. Things. J. 8 (14) (2021) 11123–11134, https://doi.org/10.1109/JIOT.2021.3051603. Jul.
[29] Z. Lin, Z. Feng, K. Guo, A. Nauman, D. Niyato, J. Wang, AI-driven seamless and massive access in space-air-ground integrated networks, IEEE Wirel. Commun 32 (3) (2025) 72–79, https://doi.org/10.1109/MWC.001.2400371.
[30] L. Zhi, et al., Self-powered absorptive reconfigurable intelligent surfaces for securing satellite-terrestrial integrated networks, China Commun. 21 (9) (2024) 276–291, https://doi.org/10.23919/JCC.fa.2023-0437.202409. Sep.
[31] Z. Lin, M. Lin, B. Champagne, W.P. Zhu, N. Al-Dhahir, Secrecy-energy efficient hybrid beamforming for satellite-terrestrial integrated networks, IEEE Trans. Commun. 69 (9) (2021) 6345–6360, https://doi.org/10.1109/TCOMM.2021.3088898. Sep.
[32] ITU. Radiocommunication Bureau, 2017, Propagation data and prediction methods for the planning of short-range outdoor radiocommunication systems and radio local area networks in the frequency range 300 MHz to 100 GHz, ITU-R Rec. P.1411-11, 2019. [Online]. Available: http://ael.chungbuk.ac.kr/lectures/graduate/antenna-engineering/21-2/propagation-models-data/R-REC-P.1411-9-201706-I!!PDF-E.pdf. Accessed: Jan. 7, 2026.
[33] A. Habib, S. Moh, Wireless channel models for over-the-sea communication: a comparative study, Appl. Sci. 9 (2019) 443, https://doi.org/10.3390/APP9030443. *Page*vol. 9, no. 3, p. 443, Jan. 2019.
[34] F.S. Alqurashi, A. Trichili, N. Saeed, B.S. Ooi, and M.-S. Alouini, “Maritime Communications: a survey on enabling technologies, opportunities, and challenges,” Apr. 2022, [Online]. Available: http://arxiv.org/abs/2204.12824.
[35] Y. Liang, N. Gao, T. Liu, Suppression method of inter-symbol interference in communication system based on mathematical chaos theory, J. King Saud Univ. Sci 32 (2) (2020) 1749–1756, https://doi.org/10.1016/j.jksus.2020.01.012. Mar.
[36] J. Liu, Y. Yan, H. Yu, B. Ma, Approximate BER performance of LoRa modulation with heavy multipath interference, IEEE Wirel. Commun. Lett. 12 (5) (2023) 853–857, https://doi.org/10.1109/LWC.2023.3246132. May.
[37] L. Wang, M.M. Wang, Interleaved chirp spreading LoRa-based modulation with continuous phase, IEEE Commun. Lett. 29 (5) (2025) 873–877, https://doi.org/10.1109/LCOMM.2024.3482276.
[38] ITU-R, “Propagation in short-range outdoor radiocommunication systems.,” 2025. [Online]. Available: https://www.itu.int/publ/R-REC/en.
[39] N. Jovalekic, V. Drndarevic, E. Pietrosemoli, I. Darby, M. Zennaro, Experimental study of LoRa transmission over seawater, Sens. (Switz.) 18 (9) (2018), https://doi.org/10.3390/s18092853. Sep.
[40] M.S. Philip, P. Singh, Adaptive transmit power control algorithm for dynamic LoRa nodes in water quality monitoring system, in: Sustainable Computing: Informatics and Systems 32, 2021, https://doi.org/10.1016/j.suscom.2021.100613. Dec.
[41] A. Farhad, J.Y. Pyun, LoRaWAN Meets ML: A Survey on Enhancing Performance with Machine Learning, Multidisciplinary Digital Publishing Institute (MDPI), 2023, https://doi.org/10.3390/s23156851. Aug. 01.